

Synthesis, crystal structures and electronic properties of imidazoline nitroxide radicals bearing active groups in electropolymerisation

Eugenio Coronado,^a Carlos Giménez-Saiz,^a Mael Nicolas,^a Francisco M. Romero,^{*a} Eduard Rusanov^b and Helen Stoeckli-Evans^b

^a Institut de Ciència Molecular, Universitat de València, Dr. Moliner 50, E-46100, Burjassot, Spain. E-mail: fmrn@uw.es; Fax: +34 9 6354 4859; Tel: +34 9 6354 4859

^b Institut de Chimie, Université de Neuchâtel, 51 Av. de Bellevaux, CH-2000, Neuchâtel, Switzerland

Received (in Montpellier, France) 6th September 2002, Accepted 23rd November 2002

First published as an Advance Article on the web 4th February 2003

Thiophene-, phenylthiophene-, and indole-based nitronyl nitroxide (NN) and imino nitroxide (IN) radicals have been synthesised and their electrochemical and magnetic properties have been studied. Cyclic voltammetry measurements show that NN radicals (**1–3**) exhibit a one-electron quasi-reversible oxidation process that results in the formation of the corresponding nitrosonium cations. This behaviour pushes the oxidation potential of the other redox-active moiety to very high values. The oxidation of the thiophene subunit occurs at 2.35 V, whereas the oxidation of the phenylthiophene and indole moieties takes place at 1.65 and 1.39 V, respectively. Oxidation of IN radicals (**4–5**) is irreversible and occurs at higher potentials, as compared to the parent NN compounds. This process has a weaker effect on the redox behaviour of the thiophene functions. Single-electron reductions are observed for all the radicals at around -1.2 V. The thiophene-based NN radical (**1**) crystallises in the monoclinic $C2/c$ space group. The analysis of the crystal structure shows the formation of dimers of molecules related by a centre of symmetry. These dimers packed to form a honeycomb lattice of radicals. An estimate of the magnetic interaction between radicals in the solid ($J = -3.4$ K) has been obtained by fitting the magnetic susceptibility of **1** with the corresponding high-temperature series expansion. The indole-based NN radical (**3**) crystallises in the monoclinic $P2_1/n$ space group. The crystal packing shows the presence of strong hydrogen bonds between the nitroxide oxygen atom and the hydrogen of the indolic amino function. This leads to zigzag chains that packed in the solid to form a two-dimensional squared lattice. Using the high-temperature series expansion for a 2D squared lattice of isotropic $S = 1/2$ spins in the fit of the magnetic susceptibility of **3** affords a value of $J = -0.11$ K for the interrational exchange coupling parameter. The phenylthiophene-based IN compound (**5**) crystallises in the triclinic $P1$ space group. Three independent molecules form its crystal structure. The magnetic properties of compounds **2**, **4** and **5** are also indicative of weak antiferromagnetic interactions. Curie–Weiss plots for these compounds afford values of the Weiss constant θ of -1.5 , -2.8 and -1.9 K for **2**, **4** and **5**, respectively.

Introduction

The preparation of magnetic polymers, or magnetically responsive organic polymeric substances, has been a subject of interest for a long time. In 1967, Keana *et al.* reported the synthesis and ESR properties of the first paramagnetic polymer bearing stable free radicals as pendant groups.¹ More recently, numerous reports claiming ferromagnetic behaviour in organic polymers have appeared in the literature. However, these materials usually have ill-defined compositions and very low values of the saturation magnetisation, so that their magnetic properties have often been ascribed to the presence of iron oxide impurities.² To date, there is no reference on the preparation of a polymer with a well-defined ferromagnetic behaviour and several groups are still interested in this challenge.

The strategies that are currently used in the design of such a material rely on the topological rules formerly applied for the construction of high-spin molecules.³ This approach concerns a series of π -conjugated alternant molecules called “non-Kekulé-molecules”.⁴ A conjugated system is called alternant if its atoms can be subdivided into two groups, denoted $A\uparrow$ and $A\downarrow$, so that each $A\uparrow$ atom is surrounded by $A\downarrow$ atoms, and vice versa. For such a system, a Hückel-type treatment

shows that the spin quantum number (S) of the ground state is related to the molecular connectivity and equals $(|n_{A\uparrow} - n_{A\downarrow}|)/2$, where $n_{A\uparrow}$ and $n_{A\downarrow}$ are the number of carbon atoms in each group. Physically, the arrows denote the direction of the spin polarisation on each carbon atom. From Chart 1, it is easy to see that the two polyradicals **A** and **B** have been designed in such a way that the spin polarisations of the different radical centres are in phase. **A** and **B** are model systems of the two strategies that are now employed in the preparation of ferromagnetic polymers: the formation of radicals in the main backbone of the polymer⁵ (**A**) or the use of pendant radical groups⁶ (**B**). Clearly, the second approach has the advantage that the π -conjugation is not altered by the presence of spin defects. Although this idea was proposed

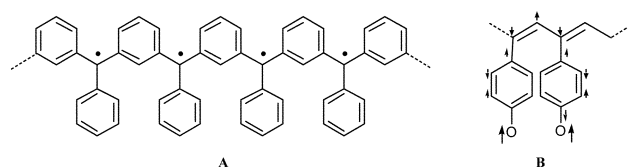
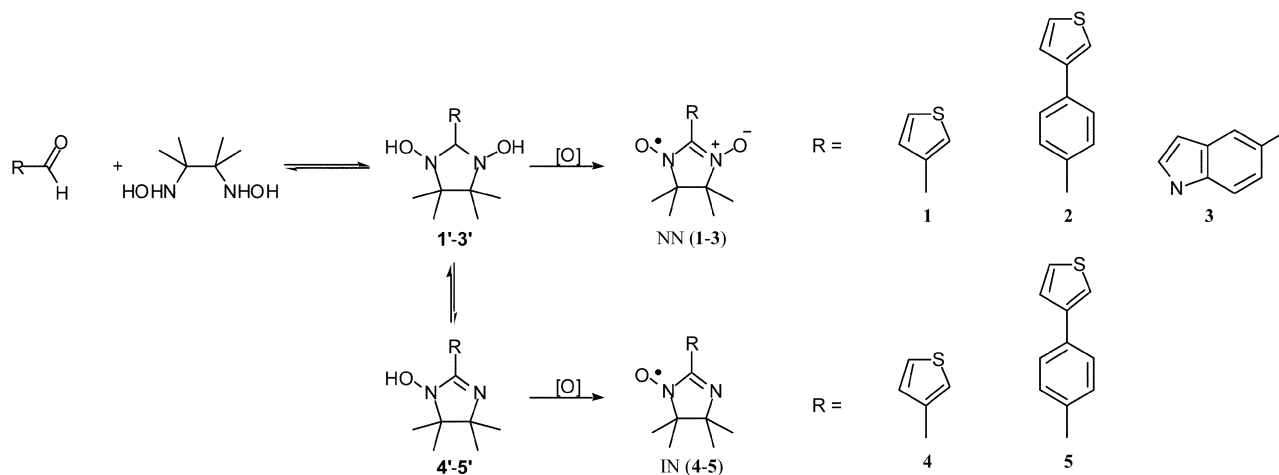


Chart 1



Scheme 1

by Ovchinnikov some twenty years ago,⁷ it is not until recently that similar polyacetylene-based radicals have been synthesised.⁸ However, the lack of planarity makes the existence of exchange interactions in these systems difficult and the most promising results have been obtained from a series of phenoxyl radicals attached to poly(phenylenevinylene), where the presence of high-spin states has been detected.⁹

Another possible strategy can result from the synthesis of thiophene or pyrrole derivatives bearing stable free radicals.¹⁰ These compounds could, in principle, be polymerised by electrochemical oxidation to give conducting polymers containing long sequences of conjugated double bonds. The conductivity of these materials is ensured by the migration along the conjugated chain of delocalised charge centres, called polarons. Thus, the presence of free radicals as pendant units in these polymers could yield materials with mobile electrons in the delocalised backbone in addition to the localised electrons of the radical species. This can result in a new family of ferromagnetic and conducting materials.

Electroactive polypyrrole films containing a nitroxide group have been prepared as electrocatalysts in alcohol oxidation reactions.¹¹ TEMPO free radicals have also been incorporated in polypyrrole matrices as spin probes of the polymeric structure.¹² Only very recently, the magnetic behaviour of these systems has been addressed. For example, one-electron oxidation of amine-based nitronyl nitroxide radicals affords cation diradicals with a triplet $S = 1$ ground state, as evidenced by ESR measurements.¹³ The magnetic and electrical properties of different radical-substituted thiophenes prepared by FeCl_3 -promoted chemical polymerisation have been studied in detail: magnetic measurements of a polythiophene bearing galvinoxyl radicals gave evidence for short-range ferromagnetic interactions between pendant units. After doping, however, no interaction between mobile and conducting electrons was observed.¹⁴

In the present work, we have attempted the direct polymerisation of nitronyl nitroxide (NN) and imino nitroxide (IN) radicals bearing electroactive groups. We herein report on the synthesis, crystal structures and electrochemical and magnetic properties of thiophene-, phenylthiophene- and indole-based NN/IN radicals.

Results and discussion

Synthesis

Nitronyl nitroxide radicals (1–3) were synthesised by double condensation of N,N' -dihydroxy-2,3-diamino-2,3-dimethyl-

butane with the corresponding aldehydes and subsequent oxidation of the condensation product (N,N' -dihydroxyimidazoline) with sodium periodate in a biphasic medium, following the method described by Ullman *et al.*¹⁵ (Scheme 1).

The parent aldehydes thiophene-3-carboxaldehyde and indole-5-carboxaldehyde are commercially available, while the compound 4-(3-thienyl)-benzaldehyde was prepared using a Suzuki-type cross-coupling reaction of 4-formyl-phenylboronic acid and 3-bromothiophene.¹⁶ The condensation reaction of thiophene-3-carboxaldehyde and N,N' -dihydroxy-2,3-diamino-2,3-dimethylbutane in methanol affords N,N' -dihydroxyimidazoline (1') as a white precipitate. In the case of the other two aldehydes, however, no precipitation was observed and the corresponding radical precursors were not isolated.

During the course of the condensation reaction partial dehydration to the corresponding N -hydroxyimidazoline can occur. In these cases, the oxidation of the crude mixture results in a mixture of radicals, from which the imino nitroxides (4, 5) can be isolated by column chromatography.

Electrochemical properties

The electrochemistry of nitronyl nitroxide (NN) radicals has been addressed in a few previous reports. Ziessel and co-workers have studied a family of oligopyridine-based bis(nitronyl nitroxides).¹⁷ It is known that the nitroxide groups are oxidised at potentials around 0.4 V (*vs.* Ag/Ag^+) by a one-electron quasi-reversible process to the nitrosonium cation. The reduction takes place irreversibly. It is believed that the nitroxide units are reduced by a one-electron process to the anions, which subsequently react with traces of water present in the solvent to form the hydroxylamines. This reaction takes place at potentials higher than -1.6 V. Electrochemical studies concerning the imino nitroxide (IN) radicals are even scarcer.

The electrochemical properties of compounds 1–5 has been studied by cyclic voltammetry (CV) and differential pulse voltammetry (DPV) measurements. The standard rate constant k_s for the mono-electronic transfer can be determined by cyclic voltammetry from the peak-to-peak separation at different scan rates. The method described by Nicholson¹⁸ is used and k_s can be estimated from the following equations:

$$k_s = \Psi(\pi a D_0)^{1/2}$$

$$a = nFv/RT$$

where Ψ is a kinetic parameter calculated from the separation between cathodic and anodic peaks, D_0 the diffusion coefficient, n the number of electrons exchanged, F the Faraday constant, v the scan rate, R the gas constant and T the

Table 1 Selected electrochemical parameters for compounds **1–5**

	$E_{\text{red}}^{\text{a}}$ V ^a	ΔE_{p} mV ^b	E_{ox}^{c} V ^c	ΔE_{p} mV ^b	k_{s} $10^{-3} \text{ cm} \cdot \text{s}^{-1}$ ^d	E_{pa} V ^e
1	−1.35	724	0.41	116	4.4	2.35
2	−1.33	463	0.39	88	9.6	1.65
3	−1.25	571	0.34	97	7.2	1.39
4	−1.24	542	0.92	—	—	1.82
5	−1.22	581	0.90	—	—	1.70

^a Average of anodic and cathodic peak potentials corresponding to the reduction of the nitroxide radical. ^b Peak-to-peak separation at a scan rate of $100 \text{ mV} \cdot \text{s}^{-1}$. ^c Average of anodic and cathodic peak potentials corresponding to the oxidation of the nitroxide radical. ^d Standard rate constant for the quasi-reversible oxidation process. ^e Irreversible oxidation peak of the aromatic electroactive group.

temperature. Table 1 quotes the voltamperometric data for all the compounds described in the present study.

For **1**, the reduction wave is observed at -1.35 V . This process is highly irreversible, with a difference between the anodic and cathodic peak potentials equal to 724 mV (Fig. 1). The oxidation takes place at 0.41 V . The formation of the nitroso-nium cation pushes the redox potential of the thiophene moiety to higher values. Thus, the irreversible oxidation wave related to this donor is seen at 2.35 V . This value falls in the potential range observed for other substituted thiophenes (from 1.57 V for 3-methylthiophene to 2.41 V for 3-nitrothiophene¹⁹). Taking into account the linear relationship between oxidation potential and Hammett constant, it can be deduced that the nitronyl nitroxide group has an electron-withdrawing character similar to that of a nitro group. Polymerisation trials at a fixed potential (higher than 2 V) or by cycling the potential in different intervals were unsuccessful. Clearly, the presence of the NN substituent as a nitrosonium ion shifts the potential of the thiophene residue to a high value, where electropolymerisation is not possible. The impossibility or difficulty to electropolymerise monomers of high oxidation potentials has been attributed to the high reactivity of the corresponding radicals, which can thus undergo rapid reactions with the solvent or anions to form soluble products.²⁰

In order to overcome this difficulty, our attention was turned to the phenylthiophene derivative **2**. The intention was to separate the thiophene and NN moieties by a conjugated spacer. This should reduce the oxidation potential of the thiophene part, maintaining some electron delocalisation in the system. In fact, the oxidation of thiophene in **2** is shifted 700 mV to lower potential as compared to **1** (Fig. 2), and takes place at 1.65 V , while the one-electron oxidation and reduction

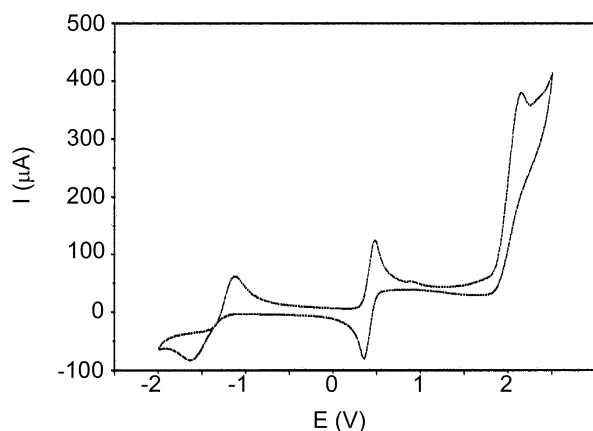


Fig. 1 Cyclic voltammogram for compound **1**, in acetonitrile with $10^{-1} \text{ M Bu}_4\text{NPF}_6$, at a scan rate of $100 \text{ mV} \cdot \text{s}^{-1}$.

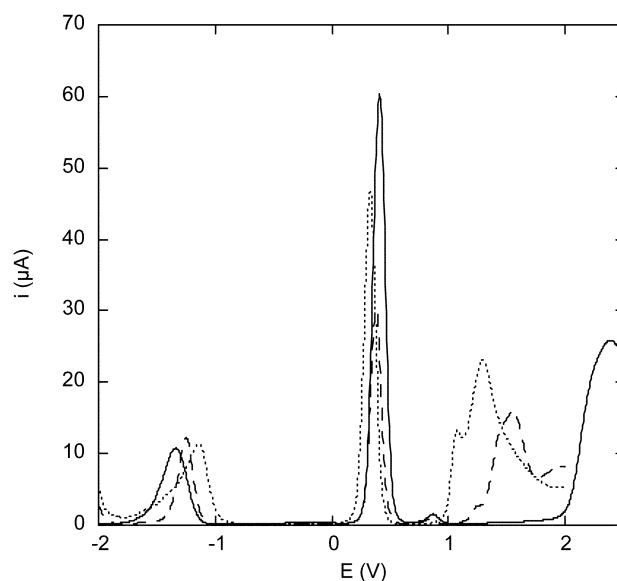


Fig. 2 Differential pulse voltammogram for compounds **1** (solid line), **2** (dashed line) and **3** (dotted line) in acetonitrile with $10^{-1} \text{ M Bu}_4\text{NPF}_6$, DPV parameters: modulation time, 0.1 s ; interval time, 1 s ; modulation amplitude, 50 mV ; scan rate, $100 \text{ mV} \cdot \text{s}^{-1}$.

potentials corresponding to the free radical unit have similar values. However, the expected deposition on the electrode of a polymeric electroactive film was not observed, independently of the cell conditions (concentration, potential range, ...).

In the case of the indole derivative **3**, a quasi-reversible oxidation process is observed at a half-wave potential of 0.34 V . This corresponds again to the formation of the nitrosonium cation. The oxidation of the indole moiety takes place at 1.39 V . It has been reported that the electrochemical oxidation of 5-substituted indoles depends strongly on the electron-withdrawing properties of the substituent and correlates well with the Hammett substituent constants.²¹ Typical potential values go from 0.98 V (for unsubstituted indole) to 1.42 V (for 5-nitroindole). From this study, it can be confirmed that the nitrosonium cation derived from a NN radical has an electron-withdrawing ability equivalent to that of a nitro group. Again, electropolymerisation failed under a wide range of conditions.

The IN radicals **4** and **5** exhibit quite similar behaviour (Fig. 3). A single-electron reduction wave is observed around -1.2 V . This is an irreversible process, with a difference of potential between the anodic and cathodic peak around 0.5 V . It can correspond to the transformation of the imino nitroxide to the hydroxyimidazoline, *via* one-electron reduction and subsequent protonation. In oxidation, a highly irreversible signal appears at 1 V . With respect to the analogue NN compounds, the oxidation reaction occurs at higher potentials and loses its reversibility, whereas the electrochemical parameters of the reduction reaction are almost the same. Interestingly, the oxidation of the IN radical has a very weak effect on the oxidation potential of the thiophene counterpart. For instance, oxidation of the thiophene moiety in **4** takes place at 1.73 V , while in the analogous NN radical **1** it occurs at potentials higher than 2 V .

Description of the structures

Thiophene-3-NN (1). This compound crystallises in the $C2/c$ centrosymmetric space group. Fig. 4 shows an ORTEP view of the molecular structure. The nitronyl nitroxide moiety features the expected bond distances and angles. The dihedral angle between the thiophene subunit and the five-membered imidazoline ring is 16.4° . This is much lower than the usual value

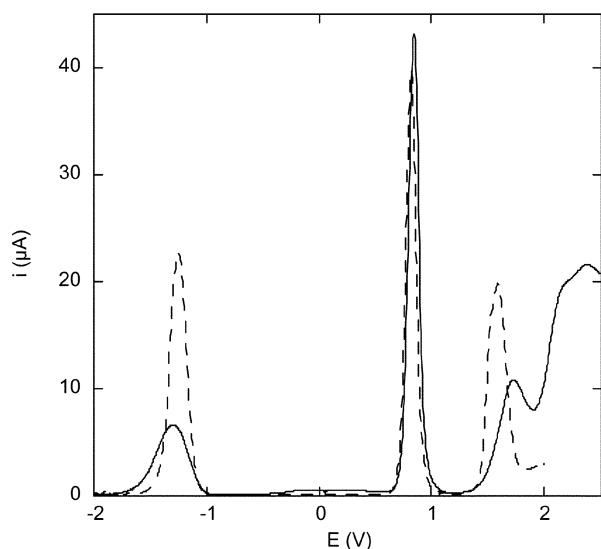


Fig. 3 Differential pulse voltammogram for compounds **4** (solid line) and **5** (dashed line) in acetonitrile with 10^{-1} M Bu_4NPF_6 , DPV parameters: modulation time, 0.1 s; interval time, 1 s; modulation amplitude, 50 mV; scan rate, 100 mV s^{-1} .

found in other heteroarene-substituted NN radicals and might be due to the fact that there is less steric repulsion between the nitroxide fragments and the protons located in the α positions of the five-membered thiophene ring. A close view of the packing shows the existence of dimeric entities, consisting of two molecular units related by an inversion centre (Fig. 5). The shortest intermolecular distance (excluding all hydrogen atoms) between these molecules is $\text{O}(1) \cdots \text{C}(1)$ ($-x, -y, -z$) = 3.286 Å. The closest interdimeric distance is also found between the oxygen atom of a nitroxide fragment and a carbon atom situated in an α position in the thiophene ring $\text{O}(2) \cdots \text{C}(4)$ ($1/2 - x, y + 1/2, 1/2 - z$) = 3.318 Å. This contact organises chains of radicals running along the y direction and links the dimeric units to form sheets of dimers that lie perpendicular to the c crystallographic axis. Each dimer is related to four adjacent dimeric units. As a result, each radical is connected to three adjacent molecules, forming a 3-connected hexagon network (honeycomb) lattice. Significant contacts are also observed between the radical moiety and the sulfur atom: $\text{O}(2) \cdots \text{S}(1)$ ($1/2 - x, y + 1/2, 1/2 - z$) = 3.350 Å. The shortest O–O distance, $\text{O}(1) \cdots \text{O}(1)$ ($-x, y, 1/2 - z$), equals 3.838 Å and also organises dimers of molecules related by a glide plane.

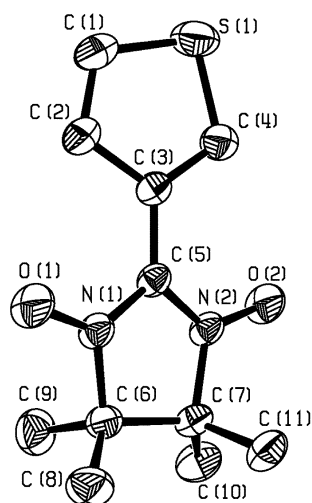


Fig. 4 ORTEP view of compound **1**.

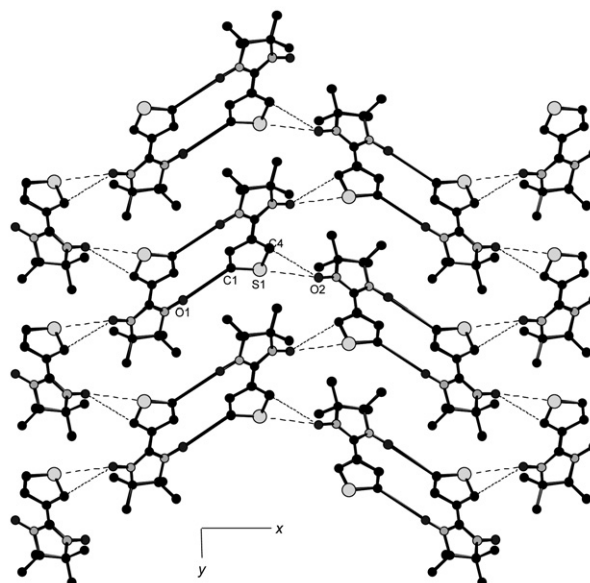


Fig. 5 View of the crystal structure of **1** along the c axis. The solid lines between the molecules emphasise the formation of dimers. Dashed lines show other intermolecular contacts.

Indole-5-NN (3). This compound crystallises in the $P2_1/n$ centrosymmetric space group. Fig. 6 shows an ORTEP view of the molecular structure. The nitronyl nitroxide moiety features the expected bond distances and angles. The dihedral angle between the thiophene subunit and the five-membered imidazoline ring is 30.0° . The crystal packing is determined by the presence of strong hydrogen bonds between a nitroxide oxygen atom and the hydrogen atoms of the indolic amino function: $\text{O}(1) \cdots \text{N}(3)$ ($x + 1/2, 1/2 - y, z + 1/2$) = 2.783 Å. The hydrogen-bonded molecules form zigzag chains that run parallel to the $[101]$ direction (Fig. 7). The shortest distances between chains have been found between the remaining oxygen atom and two methyl protons: $\text{O}(2) \cdots \text{C}(7)$ ($x - 1/2, 1/2 - y, z - 1/2$) = 3.334 Å and $\text{O}(2) \cdots \text{C}(3)$ ($x - 1/2, 1/2 - y, z - 1/2$) = 3.425 Å. A projection of this squared lattice in the bc plane shows the presence of the chains formed by hydrogen bonding (dashed lines) that lie parallel to infinite chains formed by the bifurcated $\text{C}(3) \cdots \text{O}(2) \cdots \text{C}(7)$ interaction (dotted lines). The interconnection of these chains leads to a two-dimensional structure in which each radical is connected to four adjacent molecules (2D square lattice). The nitroxide functions remain far from each other, the shortest O–O distance being $\text{O}(1) \cdots \text{O}(1)$ ($-x, -y, -z$) = 4.998 Å.

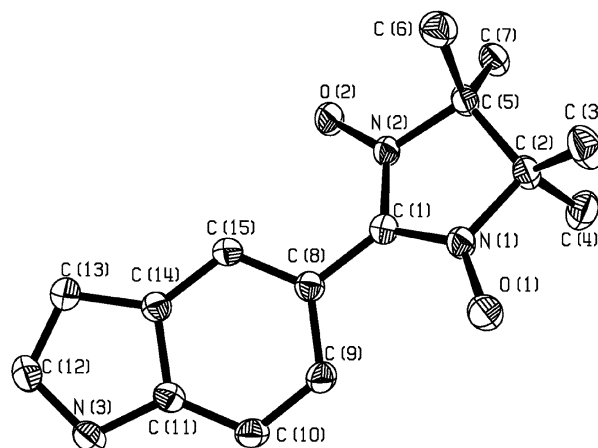


Fig. 6 ORTEP view of compound **3**.

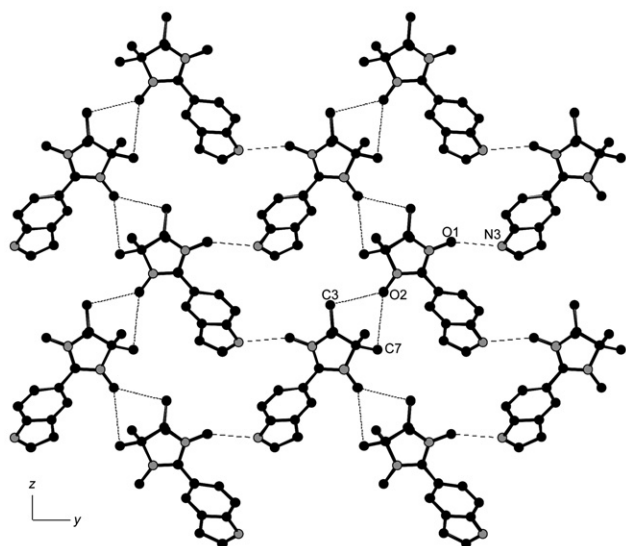


Fig. 7 View of the crystal structure of **3** along the *a* axis. Dashed lines show the hydrogen bonds. Dotted lines show other intermolecular contacts.

Phenylthiophene-4'-IN (5). This compound crystallises in the *P1* centrosymmetric space group. The crystal structure shows the presence of three independent molecules, denoted S1, S2 and S3 (Fig. 8). With respect to the relative arrangement of the sulfur atom and the nitroxide function, molecule S1 adopts a *transoid* conformation. Molecules S2 and S3 show two alternate positions for the thiophene ring. The sulfur and carbon atoms involved are split and the occupancies refined $S(2a)/S(2b) = [C(24a)/C(24b)] = 0.677/0.323$; $S(3a)/S(3b) = [C(44a)/C(44b)] = 0.727/0.273$. The bond distances involved were also constrained, with $C-S = 1.71(2)$ Å and $C-C = 1.43$ (2) Å. Molecule S3 is also disordered, with the occupancy of the nitroxide oxygen atom O(31) distributed in the two positions adjacent to nitrogen [refined occupancies: $O(31a)/O(31b) = 0.427/0.523$]. The imino nitroxide moieties feature the expected bond distances and angles. The dihedral angles between the five-membered imidazoline rings and the phenyl groups lie in the usual range (between 12.7° for S1 and 4.9° for S2) for IN radicals. The dihedral angles between

the five-membered thiophene rings and the phenyl groups lie between 18.2° (for S1) and 6.9° (for S3). The three independent molecules are connected, forming a linear trimer. Molecule S3 is related to S1 by a short contact between a nitroxide oxygen atom and the sp^2 carbon atom of the adjacent imidazoline ring: $O(1)-C(51)$ ($1+x, y, z$) = 2.994 Å. Short interatomic distances connect molecules S2 and S3 through hydrogen bonds between the oxygen atom of a nitroxide fragment and a carbon atom situated in the α position in the thiophene ring: $O(31B)-C(21) = 3.230$ Å; $O(2)-C(41) = 3.246$ Å. Other contacts shorter than 3.5 Å are found between the disordered oxygen atoms and the hydrogen atoms of the methyl groups: $O(31A)-C(17) = 3.443$ Å; $O(31B)-C(33) = 3.476$ Å. As a result, the trimers are packed around an inversion centre, forming hexamers that organise themselves into chains running along the *x* axis.

Magnetic properties

Thiophene-3-NN (1). At room temperature, the product of molar magnetic susceptibility with temperature (χT) is equal to $0.37 \text{ emu}\cdot\text{K}\cdot\text{mol}^{-1}$, the expected value for $S = 1/2$ spins in the absence of any magnetic interaction. The χT product then decreases smoothly as the sample is cooled down to 50 K. Below this temperature, χT decreases steadily on cooling and reaches a value of $0.024 \text{ emu}\cdot\text{K}\cdot\text{mol}^{-1}$ at 2 K. The susceptibility curve $\chi(T)$ shows a maximum (Fig. 9) at 5.7 K. These data point to the presence of a non-magnetic ground state, resulting from the presence of antiferromagnetic interactions between molecules. Since the analysis of the crystal structure reveals the existence of dimeric units, the magnetic susceptibility of **1** has been fitted to the Bleaney–Bowers equation.²² The best-fit value for the exchange coupling parameter is $J = -5.4$ K. An improvement of the quality of the fit can be made by introducing an interaction between dimers based on the mean-field approximation.²³ This leads to $J = -4.2$ K and $zJ' = -2.8$ K. The fact that the intradimer (J) and interdimer (zJ') exchange coupling parameters are of the same order of magnitude suggests the use of a model that takes into account both magnetic interactions. Keeping in mind the crystal packing of this compound, the susceptibility curve has been fitted by using the high-temperature series expansion for a honeycomb lattice of isotropic $S = 1/2$ spins.²⁴ The best-fit results

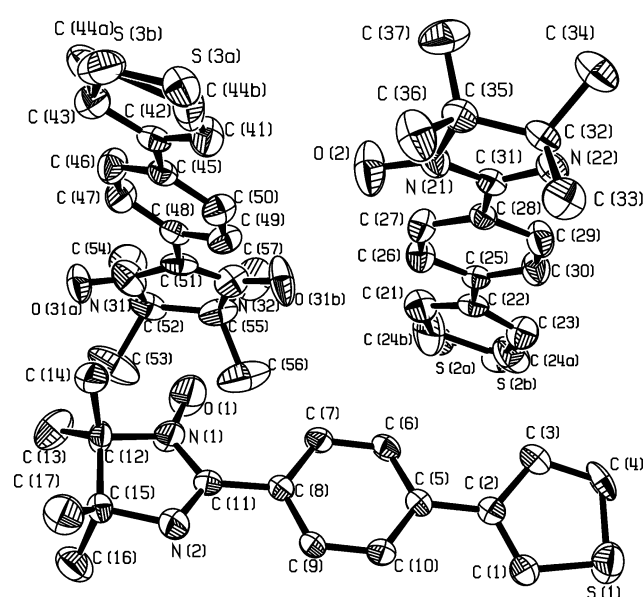


Fig. 8 ORTEP view of the three independent molecules in the crystal structure of compound **5**. Molecules have been denoted S1, S2 and S3 after their respective sulfur atom labels.

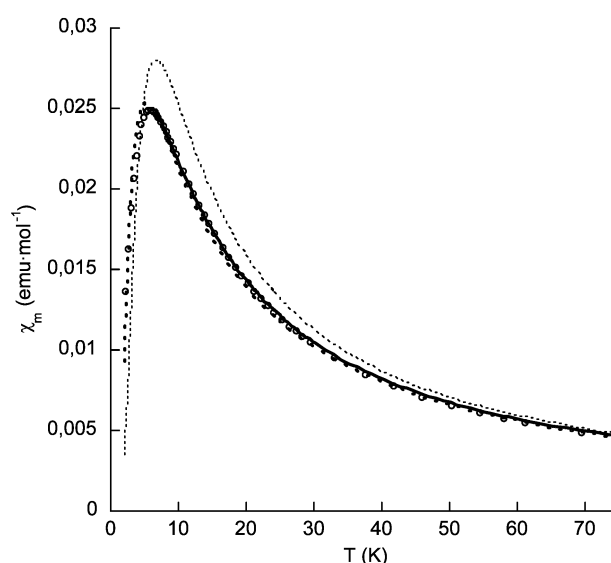


Fig. 9 Thermal dependence of the molar magnetic susceptibility of compound **1**. Open circles represent the experimental data. The dotted lines are the fits to a Bleaney–Bowers equation with (bold dotted line) and without (normal dotted line) an intermolecular mean-field term. The solid line stands for the best fit to a 2D model (honeycomb lattice).

give $J = -3.4$ K. A standard value of $g = 2.00$ has been used as a fixed constant in the different calculations.

Phenylthiophene-4'-NN (2). The χT product at room temperature ($0.31 \text{ emu}\cdot\text{K}\cdot\text{mol}^{-1}$) is slightly smaller than the expected value for non-interacting radical units. It remains constant on cooling down to 30 K (Fig. 10). Below this temperature, χT decreases continuously and reaches a value of $0.17 \text{ emu}\cdot\text{K}\cdot\text{mol}^{-1}$ at 2 K. No maximum is observed in the susceptibility curve. This indicates clearly the presence of short-range antiferromagnetic interactions between neighbouring radicals. The fit of the reciprocal susceptibility to a Curie–Weiss law affords a value of $\theta = -1.5$ K for the Weiss constant.

Indole-5-NN (3). In the 50–300 K temperature range, the product of molar magnetic susceptibility with temperature (χT) remains constant and equal to $0.36 \text{ emu}\cdot\text{K}\cdot\text{mol}^{-1}$, in close agreement with the calculated value for uncorrelated $S = 1/2$ spins. Below 50 K (Fig. 10), χT decreases smoothly on cooling and reaches a value of $0.30 \text{ emu}\cdot\text{K}\cdot\text{mol}^{-1}$ at the lowest temperature of the experiment (2 K). This behaviour is indicative of weak antiferromagnetic interactions between the spin carriers. The reciprocal susceptibility follows a Curie–Weiss law in the whole temperature range with $\theta = -0.27$ K. Keeping in mind the crystal packing of this compound, the susceptibility curve (Fig. 11) has been fitted by using the high-temperature series expansion for a square-planar lattice of isotropic $S = 1/2$ spins.²⁴ The best-fit results give $J = -0.11$ K, keeping $g = 2.00$ as a constant.

Thiophene-3-IN (4). At room temperature, the product of molar magnetic susceptibility with temperature (χT) equals $0.375 \text{ emu}\cdot\text{K}\cdot\text{mol}^{-1}$, the expected value for uncorrelated $S = 1/2$ spins. Cooling below 100 K (Fig. 10) results first in a smooth decrease of χT , then the signal decreases more sharply to reach a value of $0.12 \text{ emu}\cdot\text{K}\cdot\text{mol}^{-1}$ at the lowest temperature of the experiment (2 K). This behaviour is indicative of weak antiferromagnetic interactions between the spin carriers. The reciprocal susceptibility follows a Curie–Weiss law in the high-temperature range with $\theta = -2.8$ K. Below 7 K, there is a clear deviation from typical Curie–Weiss behaviour, indicating that the system has a low magnetic

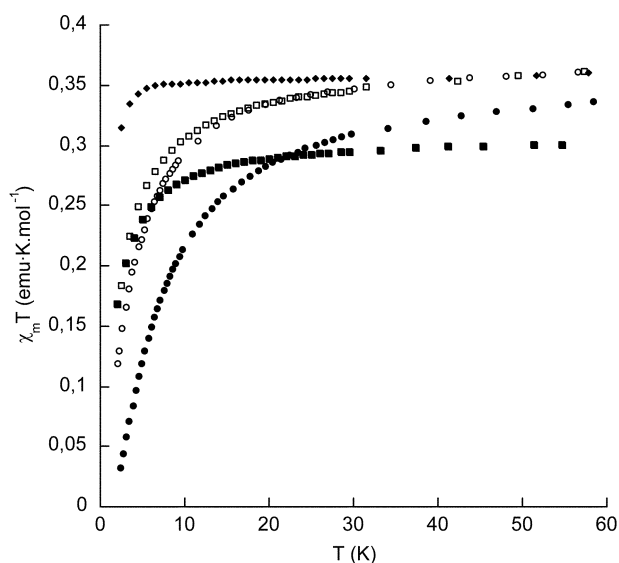


Fig. 10 Thermal dependence of the χT product of compounds 1–5: filled circles (1), filled squares (2), filled rhombuses (3), open circles (4), open squares (5).

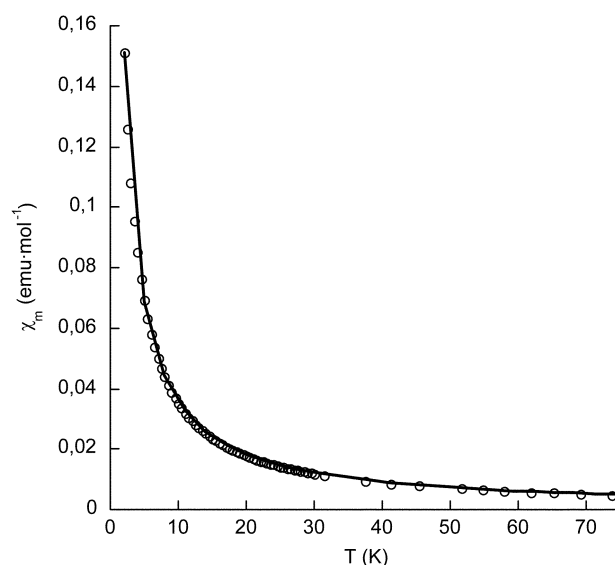


Fig. 11 Thermal dependence of the molar magnetic susceptibility of compound 3. Open circles represent the experimental data. The solid line stands for the best fit to a 2D model (square-planar lattice).

dimensionality. This fact has not been corroborated by a crystal structure analysis.

Phenylthiophene-4'-IN (5). The χT product at room temperature ($0.37 \text{ emu}\cdot\text{K}\cdot\text{mol}^{-1}$) remains constant on cooling down to 75 K, as expected for an assembly of non-interacting $S = 1/2$ spins. Below 75 K (Fig. 10), χT decreases continuously and reaches a value of $0.16 \text{ emu}\cdot\text{K}\cdot\text{mol}^{-1}$ at 2 K. This points to the presence of net antiferromagnetic interactions, even if a maximum in the susceptibility curve is not observed. The presence of three independent molecules and the existence of some disorder in the position of the N–O moiety in the crystal structure of compound 5 precludes a detailed analysis of its magnetic properties. However, the extent of the antiferromagnetic interactions can be assessed from the fit of the reciprocal susceptibility to a Curie–Weiss law. This affords a value of $\theta = -1.9$ K for the Weiss constant.

The field dependence of the magnetisation of compounds 1–5 is compared in Fig. 12 to the Brillouin curve for an $S = 1/2$ spin. All the experimental magnetisation curves deviate downwards from the Brillouin curve, confirming the fact that antiferromagnetic interactions are effective in these compounds.

Conclusion

In this paper we have reported the synthesis, electrochemical and magnetic properties of a series of NN and IN radicals conjugated to electroactive units that can undergo electropolymerisation. A large number of nitroxide radicals have been previously characterised and their magnetic properties have been studied in detail. In this work, we have also reported on their electrochemical behaviour. A relevant point is the absence of a deposited film resulting from electropolymerisation of the free radicals. This would suggest that the polymerisation process is inhibited by an inherent quenching process or that soluble oligomers are formed. For compounds 3 and 5, an exhaustive electrolytic oxidation was performed at a fixed potential (1.4 V for 3 and 1.7 V for 5). The oxidation products were analysed by electrospray ionisation mass spectrometry to verify the presence of oligomeric species in solution. The mass spectra are dominated by peaks corresponding to the electrolyte and low-weight analytes that are produced by degradation of the radicals. Oligomeric species were not detected. These

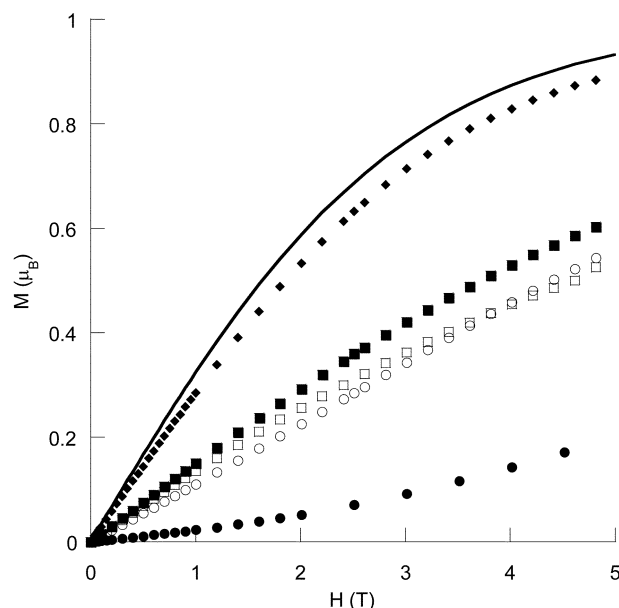


Fig. 12 Field dependence of the magnetisation of compounds **1–5** ($T = 2$ K): filled circles (**1**), filled squares (**2**), filled rhombuses (**3**), open circles (**4**), open squares (**5**). The solid line represents the expected magnetisation curve for an isolated $S = 1/2$ spin.

observations point to an effective inhibition of the polymerisation process by the free radicals.

Experimental

Electrochemical studies

Linear potential sweep cyclic and differential pulse voltammetry experiments were performed with an Autolab PGSTAT 20 apparatus (Eco Chemie B.V.) equipped with General Purpose Electrochemical System (GPES) software (version 4.5 for Windows). The working electrode was a platinum disk (surface of 1.6 mm^2). A glassy carbon rod was used as the counter electrode. All potentials are relative to the system $\text{Ag}/10^{-2} \text{ M AgNO}_3$ in acetonitrile.

The supporting electrolyte, *n*-tetrabutylammonium hexafluorophosphate (Fluka, electrochemical grade), was used as received. Acetonitrile (Fluka, anhydrous analytical grade) was used without further purification and stored under dry argon. All electrolytic solutions were degassed with argon prior to use and all experiments were carried out at room temperature.

X-Ray crystallography

Single crystals of compounds **1**, **3** and **5** suitable for X-ray analysis were obtained by slow evaporation of dichloromethane–hexane solutions. Crystallographic data for **1** were collected on a three-circle diffractometer (Bruker Smart CCD) with a CCD detector. Intensities were corrected for Lorentzian and polarisation effects. An empirical absorption correction was applied by using the SADABS²⁵ programme based on the Laue symmetry of the reciprocal space. The structure was solved by direct methods (SIR97)²⁶ and refined against F^2 with a full-matrix least-squares algorithm using SHELXL-97²⁷ and the WinGX (1.64) software package.²⁸ The 2θ range for data collection was 5.22 – 60.9° . For **3** and **5**, the intensity data were collected at 153 K on a Stoe Image Plate Diffraction System²⁹ using $\text{MoK}\alpha$ graphite monochromated radiation. Image plate distance: 70 mm; ϕ oscillation scans: 0 – 191° (**3**), 0 – 200° (**5**); step $\Delta\phi = 1.0^\circ$ (**3**), 1.5° (**5**); 2θ range: 3.27 – 52.1° ; $d_{\text{max}} - d_{\text{min}} = 12.45$ – 0.81 \AA . The structures were solved by

Table 2 Crystallographic data for compounds **1**, **3** and **5**

	1	3	5
Chemical formula	$\text{C}_{11}\text{H}_{15}\text{N}_2\text{O}_2\text{S}$	$\text{C}_{15}\text{H}_{18}\text{N}_3\text{O}_2$	$\text{C}_{17}\text{H}_{19}\text{N}_2\text{OS}$
Formula weight	239.31	272.33	299.41
Crystal system	Monoclinic	Monoclinic	Triclinic
Space group	$C2/c$	$P2_1/n$	$P\bar{1}$
$a/\text{\AA}$	23.949(2)	10.1447(8)	9.3399(9)
$b/\text{\AA}$	8.2983(9)	13.1725(8)	11.1211(12)
$c/\text{\AA}$	12.3808(13)	11.4922(8)	23.606(2)
α/deg	90	90	89.342(12)
β/deg	105.442(2)	114.697(8)	85.858(11)
γ/deg	90	90	75.866(12)
$U/\text{\AA}^3$	2371.7(4)	1395.24(17)	2371.5(4)
T/K	293(2)	153(2)	153(2)
μ/mm^{-1}	0.260	0.088	0.205
Reflections measured	9565	10 256	18 596
Reflections independent	3609	2704	8592
R_{int}	0.0301	0.0521	0.0658
$R1^a$ [$I > 2\sigma(I)$]	0.0439	0.0300	0.0747
$wR2^b$ [$I > 2\sigma(I)$]	0.1214	0.0815	0.1867

^a $R1 = \Sigma ||F_o| - |F_c|| / \Sigma |F_o|$. ^b $wR2 = [\Sigma w(F_o^2 - F_c^2)^2] / \Sigma w(F_o^2)^2]^{1/2}$.

direct methods using the programme SHELXS-97.³⁰ The refinement and all further calculations were carried out using SHELXL-97.²⁷ The H-atoms were located from Fourier difference maps and refined isotropically or included in calculated positions and treated as riding atoms using SHELXL default parameters. The non-H atoms were refined anisotropically, using weighted full-matrix least-squares on F^2 . Selected experimental parameters are given in Table 2.

CCDC reference numbers 199926–28. See <http://www.rsc.org/suppdata/nj/b2/b208762f/> for crystallographic files in CIF or other electronic format.

Materials

Commercially available (Aldrich, 98%) thiophene-3-carboxaldehyde and indole-5-carboxaldehyde were used without further purification. *N,N'*-Dihydroxy-2,3-diamino-2,3-dimethylbutane was obtained in two steps according to the literature. 4-(3-Thienyl)-benzaldehyde was prepared using a Suzuki-type cross-coupling reaction of 4-formylphenylboronic acid and 3-bromothiophene.¹⁶ Other reagents and solvents were used as purchased.

Preparations

1,3-Dihydroxy-2-(3-thienyl)-4,4,5,5-tetramethylimidazolidine (1'). Thiophene-3-carboxaldehyde (1.12 g, 10 mmol) and *N,N'*-dihydroxy-2,3-diamino-2,3-dimethylbutane (1.78 g, 12 mmol) were mixed in 100 ml of methanol, at room temperature. The reaction mixture was stirred for 24 h after which the resulting white solid was filtered off and dried under vacuum. Yield: 49%. ¹H NMR (d_6 -DMSO): δ 1.02 (s, 6H, CH_3), 1.06 (s, 6H, CH_3), 4.60 (s, 1H, CH), 7.14–7.17 (m, 1H, Hth), 7.39–7.44 (m, 2H, Hth), 7.85 (s, 2H, OH). ¹³C-¹H NMR (d_6 -DMSO): δ 17.54 (CH_3), 24.51 (CH_3), 66.38 (CCH_3), 87.08 (CH imidazolidine), 123.14, 125.38 and 128.38 (CH thiophene), 144.34 (C_{quat} thiophene). HR-MS: m/z 242.1090 [$\text{M}]^+$, calcd. for $\text{C}_{11}\text{H}_{18}\text{N}_2\text{O}_2\text{S}$: 242.1089. FT-IR (KBr): ν_{OH} 3237 cm^{-1} .

2-(3-Thienyl)-4,4,5,5-tetramethylimidazoline 3-oxide 1-oxyl (1). A solution of sodium periodate (1.28 g, 6 mmol) in 50 ml of water was added to a suspension of 1,3-dihydroxy-2-(3-thienyl)-4,4,5,5-tetramethylimidazolidine (**1'**; 1.21 g, 5 mmol) in 50 ml of dichloromethane. The biphasic mixture was stirred for 30 min at room temperature. The blue organic phase was separated, dried with MgSO_4 and concentrated under reduced pressure. The crude product was purified by

column chromatography (eluent: CH₂Cl₂–hexane, 1:1) to give **1**. Single crystals were obtained by slow evaporation of a CH₂Cl₂–hexane (1:1) solution at –20 °C. Yield: 86%. HR-MS: *m/z* 239.0850 [M]⁺, calcd. for C₁₁H₁₅N₂O₂S: 239.0854. FT-IR (KBr): ν_{NO} 1357 cm^{–1}. UV-vis (CH₂Cl₂): λ/nm ($\epsilon/\text{M}^{-1}\text{cm}^{-1}$) 570 (574), 361 (15 605), 269 (15 655).

NN radicals **2** and **3** were obtained following a similar experimental procedure. In these cases, the radical precursors were not isolated. IN radicals **4** and **5** were obtained as by-products in the synthesis of **1** and **2**, respectively, and separated from these compounds by column chromatography.

2-[4-(3-Thienyl)phenyl]-4,4,5,5-tetramethylimidazoline 3-oxide 1-oxyl (2). Yield: 20%. HR-MS: *m/z* 315.1218 [M]⁺, calcd. for C₁₇H₁₉N₂O₂S: 315.1167. FT-IR (KBr): ν_{NO} 1369 cm^{–1}. UV-vis (CH₂Cl₂): λ/nm ($\epsilon/\text{M}^{-1}\text{cm}^{-1}$) 595 (482), 375 (8556), 333 (4089), 304 (26 158), 229 (10 610).

2-(5-Indolyl)-4,4,5,5-tetramethylimidazoline 3-oxide 1-oxyl (3). Yield: 20%. HR-MS: *m/z* 272.1390 [M]⁺, calcd. for C₁₅H₁₈N₃O₂: 272.1399. FT-IR (KBr): ν_{NO} 1357 cm^{–1}, ν_{NH} 3253 cm^{–1}. UV-vis (CH₂Cl₂): λ/nm ($\epsilon/\text{M}^{-1}\text{cm}^{-1}$) 613 (1070), 367 (10 298), 295 (16 609), 254 (36 078).

2-(3-Thienyl)-4,4,5,5-tetramethylimidazoline 1-oxyl (4). Yield: 7%. HR-MS: *m/z* 223.0912 [M]⁺, calcd. for C₁₁H₁₅N₂O₂S: 223.0905. FT-IR (KBr): ν_{NO} 1365 cm^{–1}, ν_{CN} 1577 cm^{–1}. UV-vis (CH₂Cl₂): λ/nm ($\epsilon/\text{M}^{-1}\text{cm}^{-1}$) 469 (604), 333 (416), 241 (15 017).

2-[4-(3-Thienyl)phenyl]-4,4,5,5-tetramethylimidazoline 1-oxyl (5). Yield: 20%. HR-MS: *m/z* 299.1219 [M]⁺, calcd. for C₁₇H₁₉N₂O₂S: 299.1218. FT-IR (KBr): ν_{NO} 1365 cm^{–1}, ν_{CN} 1608 cm^{–1}. UV-vis (CH₂Cl₂): λ/nm ($\epsilon/\text{M}^{-1}\text{cm}^{-1}$) 458 (648), 339 (1028), 279 (30 116).

Acknowledgements

The authors gratefully acknowledge José M. Martínez-Agudo and Prof. Gómez-García for the magnetic measurements. This work was supported by the European Union (TMR ERB 4061 PL97-0197) and the Ministerio de Ciencia y Tecnología (MCT) (Programa “Ramón y Cajal”).

References

- O. H. Griffith, J. F. W. Keana, S. Rottschaefer and T. A. Warlick, *J. Am. Chem. Soc.*, 1967, **89**, 5072.
- J. S. Miller, *Adv. Mater.*, 1992, **4**, 298; J. S. Miller, *Adv. Mater.*, 1992, **4**, 435.
- H. Nishide, *Adv. Mater.*, 1995, **7**, 937.
- W. T. Borden, H. Iwamura and J. A. Berson, *Acc. Chem. Res.*, 1994, **27**, 109.
- A. Rajca, *Chem. Rev.*, 1994, **94**, 871.
- H. Nishide, T. Kaneko, S. Toriu, Y. Kuzumaki and E. Tsuchida, *Bull. Chem. Soc. Jpn.*, 1996, **69**, 499.
- A. A. Ovchinnikov, *Theor. Chim. Acta*, 1978, **47**, 297.
- A. Fujii, T. Ishida, N. Koga and H. Iwamura, *Macromolecules*, 1991, **24**, 1077; H. Nishide, T. Kaneko, N. Yoshioka, H. Akiyama and E. Tsuchida, *Macromolecules*, 1993, **26**, 4567.
- H. Nishide, T. Kaneko, T. Nii, K. Katoh, E. Tsuchida and P. M. Lahti, *J. Am. Chem. Soc.*, 1996, **118**, 9695.
- J. A. Crayston, A. Iraqi and J. C. Walton, *Chem. Soc. Rev.*, 1994, 147.
- G. Bidan and D. Limosin, *Ann. Phys.*, 1986, **11**, 5; W. F. DeGiovani and A. Deronzier, *J. Chem. Soc., Chem. Commun.*, 1992, 1461.
- P. Rapt, A. Bartl and L. Dunsch, *Polym. Bull.*, 1996, **37**, 751; P. Rapt, A. Bartl and L. Dunsch, *Synth. Met.*, 1997, **84**, 187.
- H. Sakurai, A. Izuoka and T. Sugawara, *J. Am. Chem. Soc.*, 2000, **122**, 9723; J. Nakazaki, M. M. Matsushita, A. Izuoka and T. Sugawara, *Mol. Cryst. Liq. Cryst.*, 1997, **306**, 81.
- M. Miyasaka, T. Yamazaki, E. Tsuchida and H. Nishide, *Polyhedron*, 2001, **20**, 1157.
- E. F. Ullman, J. H. Osiecki, D. G. B. Boocock and R. Darcy, *J. Am. Chem. Soc.*, 1972, **94**, 7049; E. F. Ullman, L. Call and J. H. Osiecki, *J. Org. Chem.*, 1970, **35**, 3623.
- D. F. O'Shea and J. T. Sharp, *J. Chem. Soc., Perkin Trans. 1*, 1995, 515.
- R. Ziessel, G. Ulrich, R. C. Lawson and L. Echegoyen, *J. Mater. Chem.*, 1999, **9**, 1435.
- R. S. Nicholson, *Anal. Chem.*, 1965, **37**, 1351.
- R. J. Waltman and J. Bargon, *Can. J. Chem.*, 1986, **64**, 76.
- J. Roncali, *Chem. Rev.*, 1992, **92**, 711.
- L. J. Kettle, S. P. Bates and A. R. Mount, *Phys. Chem. Chem. Phys.*, 2000, **2**, 195.
- B. Bleaney and K. D. Bowers, *Proc. R. Soc. London, Ser. A*, 1952, 214.
- A. Bino, D. C. Johnston, D. P. Goshorn, T. R. Halbert and E. I. Stiefel, *Science*, 1988, **241**, 1479.
- R. Navarro, in *Magnetic Properties of Layered Transition Metal Compounds*, ed. L. J. De Jongh, Kluwer Academic Publishers, Dordrecht, The Netherlands, 1990.
- SADABS: G. M. Sheldrick, University of Göttingen, Göttingen, Germany, 1996.
- A. Altomare, M. C. Burla, M. Camalli, G. Cascarano, C. Giacovazzo, A. Guagliardi, A. G. G. Moliterni, G. Polidori and R. Spagna, *J. Appl. Crystallogr.*, 1999, **32**, 115.
- SHELXL-97: G. Sheldrick, University of Göttingen, Göttingen, Germany, 1999.
- L. J. Farrugia, *J. Appl. Crystallogr.*, 1999, **32**, 837.
- IPDS Software, Stoe & Cie GmbH, Darmstadt, Germany, 2000.
- G. M. Sheldrick, *Acta Crystallogr., Sect. A*, **46**, 467.